DALTON
FULL PAPER

Hole states in $(Cd_{0.5}Pb_{0.5})Sr_2(Ca_xY_{1-x})Cu_2O_7$ studied by X-ray absorption spectroscopy

Ru-Shi Liu,*,†,[a] Tony Yu,[b] Jin-Ming Chen[c] and Huann-Jih Lo[b]

[a] *Department of Chemistry, National Taiwan University, Taipei, Taiwan, R.O.C.*
[b] *Department of Geology, National Taiwan University, Taipei, Taiwan, R.O.C.*
[c] *Synchrotron Radiation Research Center (SRRC), Hsinchu, Taiwan, R.O.C.*

The hole distribution of underdoped and optimum doped states in $(Cd_{0.5}Pb_{0.5})Sr_2(Ca_xY_{1-x})Cu_2O_7$ compounds has been investigated by high-resolution oxygen K-edge and copper L-edge X-ray absorption near-edge-structure spectra. Near the oxygen 1s edge, a pre-edge peak with a maximum at ≈528.3 eV was found, which is ascribed to the excitations of oxygen 1s electrons to 2p hole states located in the CuO_2 planes. The intensity of this pre-edge peak increased with calcium doping for $0 \leqslant x \leqslant 0.5$. This demonstrates that the chemical substitution of Ca^{2+} for Y^{3+} in $(Cd_{0.5}Pb_{0.5})Sr_2(Ca_xY_{1-x})Cu_2O_7$ gives rise to an increase in hole concentration within the CuO_2 planes and a change from a semiconductor to a superconductor with T_c up to 30 K. The results of the copper L-edge absorption are consistent with those observed for oxygen 1s X-ray absorption.

After the discovery of the Cd-containing 1212-type superconductors having the formula $(Cd,Pb)Sr_2(Ca,Y)Cu_2O_7$,[1,2] a number of studies of chemical substitution effects and the crystal structure[3–8] were reported. The Cd^{2+} ion is particularly interesting since its ionic radius and number of valence electrons are similar to those of Hg^{2+} [0.95 Å for Cd^{2+} and 1.02 Å for Hg^{2+} (co-ordination number = 6)[9] and 4d[10] for Cd^{2+} and 5d[10] for Hg^{2+}] which has been shown to have the highest T_c up to 135 K among the high-T_c cuprates.[10] The crystal structure of $(Cd,Pb)Sr_2(Ca,Y)Cu_2O_7$ resembles that of $YBa_2Cu_3O_7$ with the rock salt-type (Cd,Pb)O layers replacing the perovskite-type CuO chains, Sr replacing Ba, and Ca replacing a part of Y, as shown in Fig. 1. It is also recognized that the calcium content in the (Y,Ca) sites is a key factor in controlling the superconducting properties of the $(Cd_{0.5}Pb_{0.5})Sr_2(Ca_xY_{1-x})Cu_2O_7$ phase.[5]

It has been experimentally demonstrated that hole states play a pivotal role for superconductivity in the p-type cuprate superconductors. Therefore, a knowledge of the unoccupied electronic structure near the Fermi level of these compounds is an important step toward comprehensive understanding of the mechanism of superconductivity. The X-ray absorption spectra are determined by electronic transitions from a selected atomic core level to the unoccupied electronic states near the Fermi level. X-Ray absorption near edge structure (XANES) is therefore a direct probe of the character and local density of hole states responsible for high-T_c superconductivity. The availability of third-generation synchrotron radiation X-ray sources makes it feasible to measure high-signal-to-noise-ratio and high-resolution X-ray absorption spectra.

It is generally agreed that hole states in the p-type cuprates are localized on the oxygen sites. Moreover, there are generally several inequivalent oxygen sites in the superconducting cuprates. Therefore, it is important to understand the hole distribution among different sites and their role for superconductivity. However, such studies are still in infancy. We have therefore systematically investigated a series of $(Cd_{0.5}Pb_{0.5})Sr_2(Ca_xY_{1-x})Cu_2O_7$ for $x = 0$–0.5 with various hole concentrations in order to extract information concerning how the hole states affect superconducting properties in high-T_c cuprates.

† E-Mail: rsliu@ccms.ntu.edu.tw

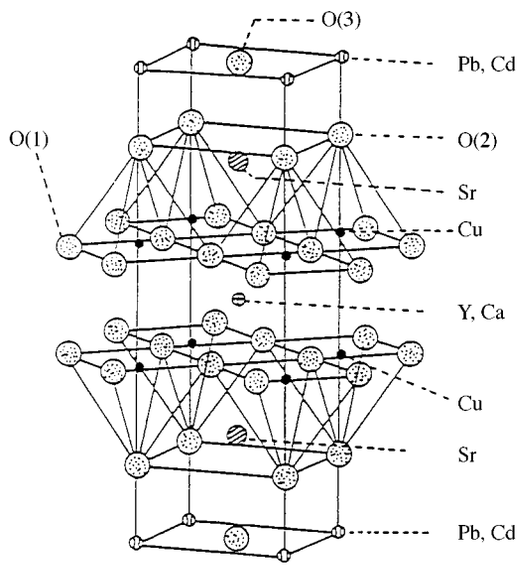

Fig. 1 Schematic crystal structure of $(Cd_{0.5}Pb_{0.5})Sr_2(Ca_xY_{1-x})Cu_2O_7$

Experimental

High-purity powders of CdO, PbO, $SrCO_3$, $CaCO_3$, Y_2O_3 and CuO were weighted in the appropriate proportions to form nominal compositions of $(Cd_{0.5}Pb_{0.5})Sr_2(Ca_xY_{1-x})Cu_2O_7$. The mixed powders were calcined at 850 °C for 15 h in air then pulverized and pressed into pellets (10 mm in diameter and 3 mm in thickness) under a pressure of 5×10^3 kg cm^{-2}. The pellets were sintered at 950 °C for 10 h in air and then cooled to room temperature. Powder X-ray diffraction (XRD) analyses were performed with a SCINTAG (XI) X-ray diffractometer (Ni-filtered Cu-Kα radiation). All the samples with $x = 0$–0.5 are single phase. When $x > 0.5$ an impurity phase appeared in the samples. Low field magnetization data were taken from a superconducting quantum interference device (SQUID) magnetometer (Quantum Design). The induced superconductivity up to 30 K was observed for the $x = 0.5$ sample. However, the $x = 0$–0.4 samples did not show any superconductivity in the temperature range 5–300 K.

The X-ray absorption measurements were carried out on the 6 m high-energy spherical grating monochromator (HSGM) beamline of the Synchrotron Radiation Research Center (SRRC) in Taiwan. Spectra recorded by total X-ray fluorescence yield mode were measured using a microchannel plate (MCP) detector.[11] This detector consists of a dual set of MCPs with an electrically isolated grid mounted in front of them. The X-ray fluorescence yield measurement is strictly bulk sensitive with a probing depth of thousands of ångströms. During these measurements the grid was set to 100 V while the front of the MCPs was set to −2000 V and the rear to −200 V. The grid bias insured that positive ions would not be detected while the negative MCP bias insured that no electrons were detected. The MCP detector was located ≈2 cm from the sample and oriented parallel to the sample surface. Photons were incident at an angle of 45° with respect to the sample normal. The incident photon intensity (I_0) was measured simultaneously by a nickel mesh located after the exit slit of the monochromator. All the absorption spectra were normalized to I_0. The photon energies were calibrated with an accuracy of 0.1 eV (eV ≈ 1.6×10^{-19} J) using the known oxygen K-edge and copper L_3-edge absorption peaks of CuO. The energy resolution of the monochromator was set to ≈0.22 and ≈0.45 eV for the oxygen K-edge and copper L-edge X-ray absorption measurements, respectively. All the measurements were carried out at room temperature.

Results and Discussion

Oxygen K-edge XANES

Based on the strong similarity of oxygen 1s absorption spectra and resonant high-energy inverse photoemission spectra of $Bi_2Sr_2CaCu_2O_8$, it is suggested that the core-hole effect in the oxygen K-edge X-ray absorption near-edge structure spectrum of the cuprate superconductors can be ignored.[12] Furthermore, according to the dipole selection rules, only the local unoccupied states with oxygen 2p character are probed in the oxygen K-edge X-ray absorption spectra. Therefore, if the hole states near the Fermi level in the p-type cuprates are of primarily oxygen 2p character, a pre-edge peak should be observable in the oxygen 1s XANES spectrum with an intensity proportional to the 2p hole concentration.

In Fig. 2 we show the oxygen K-edge X-ray absorption near-edge structure spectra for the series of $(Cd_{0.5}Pb_{0.5})Sr_2(Ca_xY_{1-x})Cu_2O_7$ samples with $x = 0$, 0.1, 0.2, 0.3, 0.4 and 0.5 in the energy range of 525–555 eV obtained by the bulk-sensitive total X-ray-fluorescence yield technique. The spectrum of the sample with $x = 0$, mainly consists of a peak at ≈530 eV and a broad peak at ≈537 eV. The spectra for the compounds can be divided into two regions: below and above photon energy ≈532 eV. The low-energy part, which consists of pre-edge peaks, is attributed to the transitions from the oxygen 1s core electron to hole states with the 2p symmetry on the oxygen sites. Based on inverse photoemission studies, the empty d states of Ca, Y and Sr are all located at least about 5–10 eV above the Fermi level.[13] Therefore, the transitions from oxygen 1s electrons to these empty d states hybridized with oxygen 2p states are probably responsible for the main absorption peak at ≈537 eV. The spectra for the various compounds with different x values in Fig. 2 were normalized to have the same height at the main peak of ≈537 eV.

As the calcium doping increases, a new pre-edge peak arises at ≈528.3 eV (marked by the arrows in Fig. 2). Based on the recent studies of the electronic structures of $HgBa_2Ca_{n-1}Cu_nO_{2n+2+\delta}$ compounds for $n \leqslant 3$, Pellegrin *et al.*[14] assigned the low-energy pre-edge peak at ≈528.2 eV to oxygen 2p hole states within the CuO_2 planes. This assignment was supported by polarized X-ray absorption measurements on a single crystal of $HgBa_2Ca_3Cu_4O_{10+\delta}$.[14] Furthermore, from

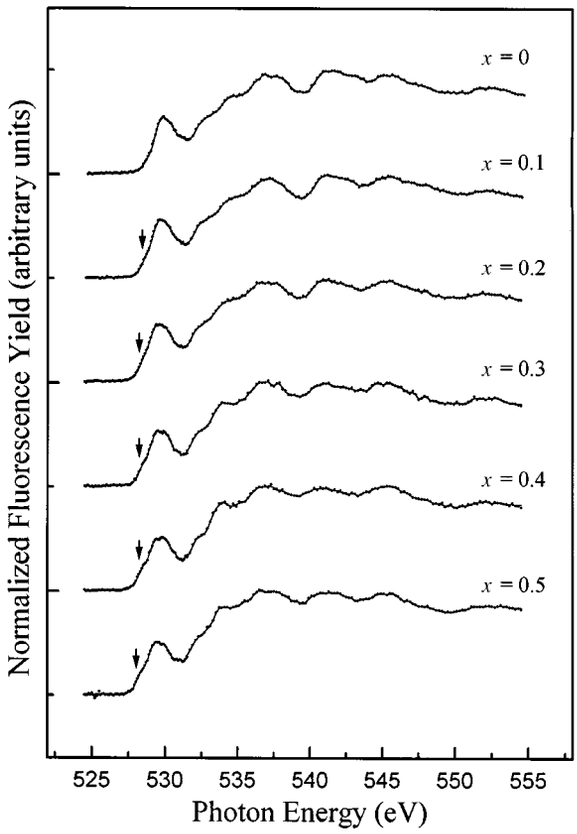

Fig. 2 Oxygen K-edge X-ray absorption near-edge structure spectra for the series of $(Cd_{0.5}Pb_{0.5})Sr_2(Ca_xY_{1-x})Cu_2O_7$ samples in the energy range 525–555 eV obtained by the bulk-sensitive total X-ray fluorescence yield technique

X-ray photoemission spectroscopy studies on the oxygen 1s core levels of epitaxial $HgBa_2CaCu_2O_{6+\delta}$ films, the oxygen 1s binding energy on the CuO_2 planes is smaller than that in the BaO layers.[15] The structural arrangement of $(Cd_{0.5}Pb_{0.5})Sr_2(Ca_xY_{1-x})Cu_2O_7$ is similar to that of $HgBa_2CaCu_2O_{6+\delta}$. We therefore adopt the same assignment in the discussion of the present data. In analogy to results from other p-type cuprate superconductors,[14,16,17] the pre-edge peak at ≈528.3 eV in Fig. 3 for the series of $(Cd_{0.5}Pb_{0.5})Sr_2(Ca_xY_{1-x})Cu_2O_7$ samples can be ascribed to excitations of oxygen 1s electrons to 2p holes located in the CuO_2 planes. It should be pointed out that the hybridization between O and Cu atoms leads to mixing between the oxygen 2p states and the copper 3d conduction band.

For most cuprate superconductors the lowest binding energies for the oxygen 1s states have been found to be between 528.5 and 529.0 eV.[18,19] It is reasonably assumed that the lowest binding energies for these states in the present compounds are also in the same range. In addition, the core-hole effect in the oxygen 1s absorption spectrum can be neglected. Therefore, the broad peak at ≈530 eV in the oxygen K-edge absorption spectrum implies that above the semiconducting gap the conduction-band states must have considerable oxygen 2p character. Therefore, one possible final state associated with the transition at ≈530 eV is the upper Hubbard band of the copper 3d states highly hybridized with the oxygen 2p states. Owing to strong on-site correlation on the copper sites in the cuprate compounds, such a band has always been assumed to exist.[20] However, another possible contribution to this peak is due to the transitions to the oxygen 2p hole states originating from the SrO and (Cd,Pb)O planes.[14] Therefore, the broad peak at ≈530 eV may be due to a superposition of unoccupied oxygen 2p states originating from the SrO and (Cd,Pb)O layers and the upper Hubbard band.

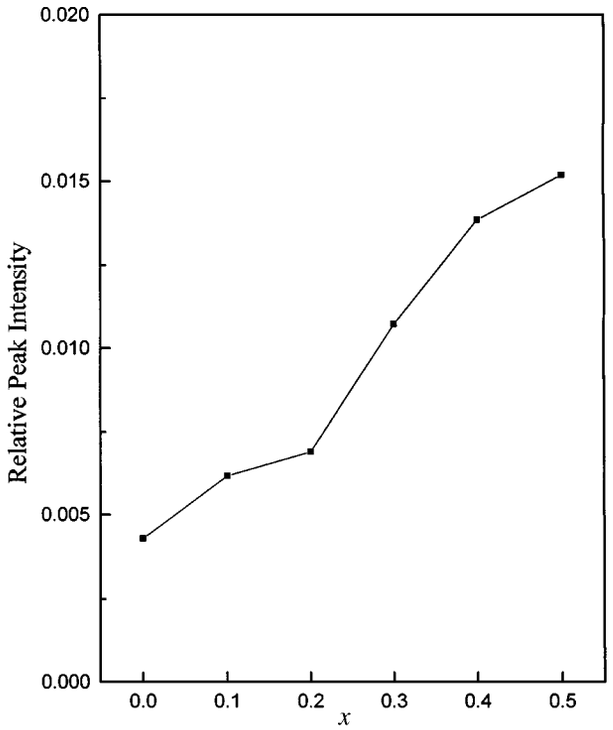

Fig. 3 The integrated intensity of the pre-edge peak at ≈528.3 eV, normalized against the intensity of main peak at ≈537 eV, as a function of calcium content x in $(Cd_{0.5}Pb_{0.5})Sr_2(Ca_xY_{1-x})Cu_2O_7$

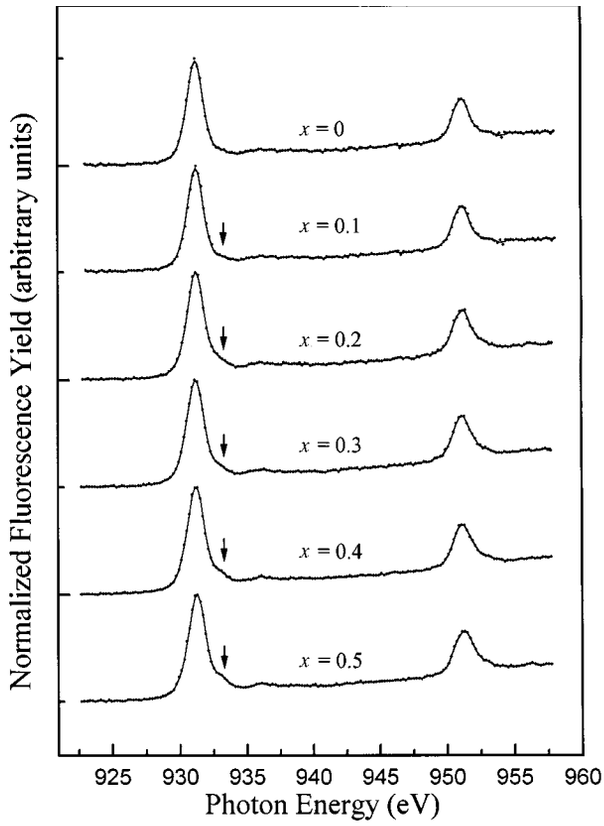

Fig. 4 Copper L_{23}-edge X-ray absorption near-edge-structure total-X-ray-fluorescence-yield spectra of $(Cd_{0.5}Pb_{0.5})Sr_2(Ca_xY_{1-x})Cu_2O_7$ in the energy range 922–958 eV

In order to investigate the variation of hole contents among different oxygen sites as a function of calcium doping, the absorption features shown in Fig. 2 were analysed by fitting Gaussian functions to each spectrum. The integrated intensity of the pre-edge peak at ≈528.3 eV, normalized against the intensity of main peak at ≈537 eV, is plotted in Fig. 3 as a function of calcium content x in $(Cd_{0.5}Pb_{0.5})Sr_2(Ca_xY_{1-x})Cu_2O_7$. The intensity of this pre-edge peak increases with increasing doping level of Ca^{2+} substituted at the Y^{3+} sites. This indicates that chemical substitution of low-valent Ca^{2+} for high-valent Y^{3+} gives rise to oxygen 2p hole states within the CuO_2 planes near the Fermi level. However, the curve could not be fitted as a simple straight line and a discrepancy at $x = 0.2$ was found which may imply that defect compensation is occurring in the samples. It should be pointed out that the system goes through a transition from a semiconductor to a superconductor at $x = 0.5$. It is therefore proposed that, at low levels of calcium doping, the hole states are localized close to the substitution site and there is a negligible overlap between the bound-state wavefunction. At high levels of doping, corresponding to the introduction of more hole states, the overlap of the wavefunctions of the acceptor states will result in charge delocalization as the system moves through an insulator (or semiconductor) to a superconductor transition. A related model has been proposed by Jarrell *et al.*[21] who have described a phenomenological model of the magnetic properties of $La_{2-x}Sr_xCuO_4$. Therefore, the generation of oxygen 2p holes within the CuO_2 planes is probably responsible for inducing a transition from a semiconductor to a superconductor. In addition, this pre-edge for $x = 0.1$ in Fig. 2 shifts by 0.1–0.2 eV to lower energies as the calcium content increases. The same behaviour of the low-energy pre-edge peak has been observed for $La_{2-x}Sr_xCuO_4$ compounds which can be considered as characteristic for the p-type cuprate superconductors.[22] In this respect, the present compounds are typical of a hole-doped cuprate superconductor.[23,24] A similar behaviour in the oxygen 1s X-ray absorption spectra with the doping concentration of Ca^{2+} in the Y^{3+} sites was reported for $(Tl_{0.5}Pb_{0.5})Sr_2(Ca_{1-x}Y_x)Cu_2O_8$ compounds.[25]

Copper L-edge XANES

The copper L_{23}-edge X-ray absorption near-edge-structure total-X-ray-fluorescence-yield spectra of $(Cd_{0.5}Pb_{0.5})Sr_2(Ca_xY_{1-x})Cu_2O_7$ with $x = 0$–0.5 in the energy range 922–958 eV are shown in Fig. 4. For $x = 0$ the spectrum shows two narrow peaks centered at 931.2 and 951.0 eV. These strong excitonic peaks are very close to the L_{23} peaks observed in the copper L_{23}-edge X-ray absorption spectrum of CuO and are attributed to transitions from the $Cu(2p^3_{2,2}^1)\ 3d^9$–$O\ 2p^6$ ground states to the $Cu(2p^3_{2,2}^1)^{-1}\ 3d^{10}$–$O\ 2p^6$ excited states, where $(2p^3_2)^{-1}$ and $(2p^1_2)^{-1}$ denote a $2p^3_2$ hole and $2p^1_2$ hole, respectively.[26]

For samples with increasing calcium content (*i.e.* increasing hole concentration), the absorption peaks become asymmetric and two new features appear at the high-energy side of the L_{23} peaks (marked by arrows in Fig. 4). From the curve-fitting analysis, the new features are centered at about 933.1 and 952.9 eV, respectively. In Fig. 5 the area of this high-energy shoulder, normalized against the area of the L_3 peak at 931.3 eV, is plotted as a function of the compositional parameter x in $(Cd_{0.5}Pb_{0.5})Sr_2(Ca_xY_{1-x})Cu_2O_7$. The areas were estimated by fitting the main peak and the shoulder by Gaussian functions. The normalized intensity of this high-energy shoulder increases with increasing calcium concentration. However, the curve could not be fitted as a simple straight line and a discrepancy at $x = 0.2$ was found which again may imply that defect compensation is occurring in the samples.

It is noted that the curve in Fig. 5 resembles the behavior of the pre-edge peak at ≈528.3 eV in the oxygen K-edge absorption spectra shown in Fig. 3. Therefore, it is suggested that these high-energy shoulders may originate from the oxygen 2p hole states and are assigned as transitions from the $Cu(2p^3_{2,2}^1)\ 3d^9\ \underline{L}$ ground state (formal Cu^{3+} state) to the $Cu(2p^3_{2,2}^1)^{-1}\ 3d^{10}\ \underline{L}$ excited state, where $\underline{L}$ denotes the oxygen 2p ligand hole.[27,28] Since there is only one type of copper site in the unit cell for the series $(Cd_{0.5}Pb_{0.5})Sr_2(Ca_xY_{1-x})Cu_2O_7$, these high-energy

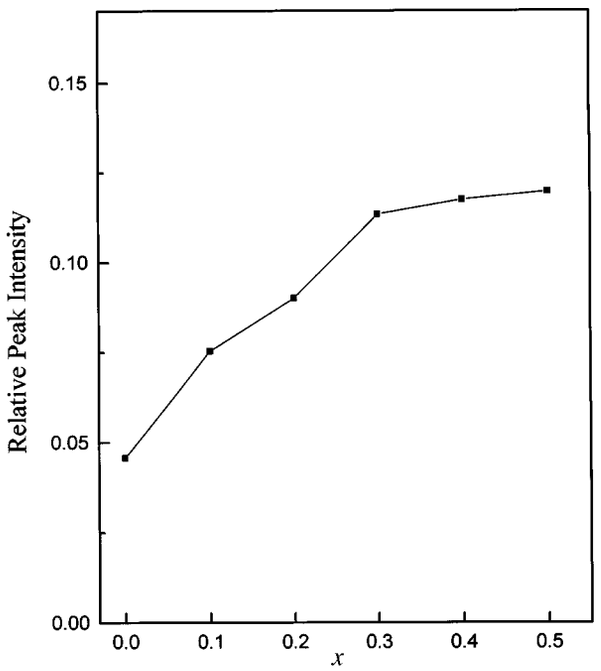

Fig. 5 Dependence on compositional parameter x in $(Cd_{0.5}Pb_{0.5})Sr_2(Ca_xY_{1-x})Cu_2O_7$ of the normalized intensity of the defect states at 933.1 eV on the copper sites

features in the copper L-edge absorption spectra can be apparently identified as a result of the hole doping within the CuO_2 layers due to the chemical substitution of Ca^{2+} for Y^{3+}. The close resemblance between the high-energy features in the copper L-edge absorption spectra and the pre-edge peak at ≈528.3 eV in the oxygen 1s absorption spectra is evidence in support of the suggestion that the pre-edge peak at ≈528.3 eV originates from the CuO_2 planes.

Conclusion

High-resolution oxygen K-edge and copper L_{23}-edge X-ray absorption near-edge-structure spectra for the series of $(Cd_{0.5}Pb_{0.5})Sr_2(Ca_xY_{1-x})Cu_2O_7$ compounds ($x = 0$–0.5) have been obtained using a bulk-sensitive total-fluorescence-yield technique. Near the oxygen 1s edge, the pre-edge peak at ≈528.3 eV is ascribed to the core-level excitations of oxygen 1s electrons to 2p holes located in the CuO_2 planes. The intensity of this pre-edge peak monotonically increases with calcium doping for $0 \leqslant x \leqslant 0.5$. This indicates that the effect of chemical substitution of Ca^{2+} for Y^{3+} is to induce hole states in the CuO_2 planes near the Fermi level. In the copper L-edge absorption spectra, high-energy shoulders at 933.1 and 952.9 eV are assigned to the transitions from the $Cu(2p^{\frac{3}{2},\frac{1}{2}})\,3d^9$ L ground state to the $Cu(2p^{\frac{3}{2},\frac{1}{2}})^{-1}\,3d^{10}$ L excited state, where L denotes the oxygen ligand hole. The normalized intensity of these defect states shows a linear increase with increasing calcium concentration. Based on the present XANES study, it is concluded that the transition from a semiconductor to a superconductor in $(Cd_{0.5}Pb_{0.5})Sr_2(Ca_xY_{1-x})Cu_2O_7$ with increase in calcium content results mainly from the increase in the hole concentration in the CuO_2 planes.

Acknowledgements

This research was financially supported by the National Science Council of the Republic of China under grant number of NSC 89-2113-M-002-005.

References

1 R. S. Liu, D. Groult, A. Maignan, S. F. Hu, D. A. Jefferson, B. Raveau, C. Michel, M. Hervieu and P. P. Edwards, *Physica C*, 1992, **35**, 195.
2 A. Maignan, D. Groult, R. S. Liu, T. Rouillon, P. Daniel, C. Michel, M. Hervieu and B. Raveau, *J. Solid State Chem.*, 1993, **102**, 31.
3 T. P. Beales, W. G. Freeman, S. R. Hull, M. R. Harrison and J. M. Parberry, *Physica C*, 1993, **205**, 383.
4 J. R. Min, J. K. Liang, X. L. Chen, C. Wang, C. Dong and G. H. Rao, *Physica C*, 1994, **229**, 169.
5 J. R. Min, J. K. Liang, X. L. Chen, C. Wang, C. Dong and G. H. Rao, *Physica C*, 1994, **230**, 389.
6 H. Jin, N. L. Wang, Y. Chong, M. Deng, K. Q. Ruan, L. Z. Cao and Z. J. Chen, *Physica C*, 1994, **231**, 167.
7 W. J. Yu, Zh. Q. Mao, C. Y. Xu, L. Yang, M. L. Tian, L. Shi, G. E. Zhou and Y. H. Zhang, *Physica C*, 1994, **234**, 151.
8 G. C. Che, F. Wu, Y. C. Lan, H. Chen, C. Dong, B. Yin, S. L. Jia and Z. X. Zhou, *Physica C*, 1995, **251**, 110.
9 R. D. Shannon, *Acta. Crystallogr.*, *Sect. A*, 1976, **32**, 751.
10 A. Schilling, M. Cantoni, J. D. Guo and H. R. Ott, *Nature* (*London*), 1993, **363**, 56.
11 J. M. Chen, S. C. Chung and R. S. Liu, *Solid State Commun.*, 1996, **99**, 493.
12 W. Wruke, F. J. Himpsel, G. V. Chandrashekar and M. W. Shafer, *Phys. Rev. B*, 1989, **39**, 7328.
13 H. M. Meyer III, T. J. Wagnener, J. H. Weaver and D. S. Ginley, *Phys. Rev. B*, 1980, **39**, 7243.
14 E. Pellegrin, J. Fink, C. T. Chen, Q. Xiong, Q. M. Lin and C. W. Chu, *Phys. Rev. B*, 1996, **53**, 2767.
15 R. P. Vasquez, M. Rupp, A. Gupa and C. C. Tsuei, *Phys. Rev. B*, 1995, **51**, 15 657.
16 J. Fink, N. Nucker, E. Pellegrin, H. Romberg, M. Alexander and M. Kunpfer, *J. Electron Spectrosc. Relat. Phenom.*, 1994, **66**, 395.
17 G. Mante, Th. Schmalz, R. Manzke, M. Skibowski, M. Alexander and J. Fink, *Surf. Sci.*, 1992, **269/270**, 1071.
18 H. M. Meyer III, T. J. Wagnener, J. H. Weaver and D. S. Ginley, *Phys. Rev. B*, 1988, **38**, 7144.
19 A. Fujimori, Y. Tokura, H. Eisaki, H. Takagi, S. Uchida and E. Takayama-Muromachi, *Phys. Rev. B*, 1990, **42**, 325.
20 D. Vaknin, S. K. Shiha, D. E. Moneton, D. C. Johnston, J. M. Newsam, C. R. Safiva and H. E. King, jun., *Phys. Rev. Lett.*, 1987, **58**, 2802.
21 M. Jarrell, D. L. Cox, C. Jayaprakash and H. R. Krishnamurthy, *Phys. Rev. B*, 1989, **40**, 8899.
22 H. Romberg, M. Alexander, N. Nucker, P. Adelmann and J. Jink, *Phys. Rev. B*, 1990, **42**, 8768.
23 P. Kuper, G. Kruizinga, J. Ghijsen, M. Grioni, P. J. Weijs, F. M. F. De Groot, G. A. Sawatzki, H. Verweij, L. F. Feiner and H. Peterson, *Phys. Rev. B*, 1988, **38**, 6483.
24 N. Nucker, J. Fink, J. C. Fuggle, P. J. Durham and W. M. Temmerman, *Phys. Rev. B*, 1988, **37**, 5158.
25 J. M. Chen, R. S. Liu and W. Y. Liang, *Phys. Rev. B*, 1996, **54**, 12 587.
26 M. Grioni, J. B. Goedkoop, R. Schoorl, F. M. F. de Groot, J. C. Fuggle, F. Schafers, E. E. Koch, G. Rossi, J. M. Esteva and R. C. Karnatak, *Phys. Rev. B*, 1989, **39**, 1541.
27 A. Bianconi, A. Congiu Castellano, M. De Santis, P. Rudolf, P. Lagarde, A. M. Flank and A. Marcelli, *Solid State Commun.*, 1987, **63**, 1009.
28 D. D. Sarma, O. Strebel, C. T. Simmons, U. Neukirch and G. Kaindl, *Phys. Rev. B*, 1988, **36**, 8285.

Received 5th *May* 1998; *Paper* 8/03355B